Electronic Supplementary Information:

Self-Optimizing Parallel Millifluidic Reactor for Scaling Nanoparticle Synthesis

Lu Wang,[a] Lanja R. Karadaghi,[b] Richard L. Brutchey,*[b] Noah Malmstadt*[abc]

[a] *Mork Family Department of Chemical Engineering and Materials Science, University of Southern California, 925 Bloom Walk, Los Angeles, California 90089-1211, United States*
[b] *Department of Chemistry, University of Southern California, 840 Downey Way, Los Angeles, California 90089-0744, United States*
[c] *Department of Biomedical Engineering, University of Southern California, 3650 McClintock Avenue, Los Angeles, California 90089-1111, United States*

E-mail: brutchey@usc.edu.
E-mail: malmstad@usc.edu.

Table of Contents

A. Experimental Procedures

A-1. Precursor preparation and product work-up

***Small-Scale (1 h reaction)*:** Cs_2CO_3 (99.9%), PbO (99.9%), and oleic acid (90%) were purchased from Sigma-Aldrich. Tetraoctylammonium bromide (TOAB) was purchased from Beantown Chemical. In a typical procedure, a 10 mM Cs^+/Pb^{2+} precursor solution was prepared by dissolving 1.0 mmol of Cs_2CO_3 and 2.0 mmol PbO in 20 mL of oleic acid under vacuum at 120 °C for 30 min. Upon cooling the mixture to room temperature, the solution was added to 200 mL of toluene. Separately, a 40 mM Br^- precursor solution was prepared by dissolving 6 mmol of TOAB in 12 mL of oleic acid and 150 mL of toluene by stirring at 1,000 rpm at room temperature. The precursor solution bottles were then assembled for use in the flow reactor, with the PTFE inlet tubing inserted directly into each precursor bottle. [**Note:** Do not dilute the Br^- precursor too much, as the driving pressures should descend along the flow stream. High pressure at downstream, i.e. gas and Br^- precursor, can sometimes lead to back flow in reactor channels]

***Large-Scale (4 h reaction)*:** The aforementioned precursor solutions were scaled up 12 × in 5-L glass bottles for the large-scale reaction. Upon preparation of the precursor solutions, the 5-L glass bottles were assembled for use in the flow reactor. After 1 h of the reaction, a 10 mL aliquot of $CsPbBr_3$ QDs was collected and split evenly between two 50-mL centrifuge tubes. The product was precipitated with 4 mL of isopropyl alcohol in each tube and briefly vortex mixed, followed by centrifugation (4,000 rpm, 5 min). The supernatant had a bright yellow tint and was discarded, leaving the yellow/green solid to be redispersed in exactly 1 mL of hexanes in each tube and briefly vortexed mixed and bath sonicated. From the 1 mL $CsPbBr_3$ QD dispersion in the first centrifuge tube, exactly 60 μL was added to a cuvette with 3 mL of hexanes for UV-vis and PL characterization. The remaining dispersion was used for XRD characterization. The second centrifuge tube with 1 mL $CsPbBr_3$ QD dispersion was centrifuged (6,000 rpm, 5 min). The bright yellow/green supernatant was used for TEM characterization.

A-2. Product characterization

***Powder X-ray Diffraction (XRD)*:** XRD patterns were acquired on a Rigaku Ultima IV diffractometer operating at 40 mA and 44 kV with a Cu $K\alpha$ X-ray source (λ = 1.5406 Å).

***Ultraviolet-Visible Spectroscopy (UV-vis)*:** UV-vis absorption data was obtained on a Perkin-Elmer spectrophotometer. The absorption data was normalized to 452 nm. The cuvette path length is 10 mm.

***Photoluminescence Spectroscopy (PL)*:** PL spectra were collected on a Horiba Jobin Yvon Nanolog spectrofluorimeter, with a photomultiplier tube detector and a 450 W Xe lamp for excitation. All samples were excited at 405 nm.

***Transmission Electron Microscopy (TEM)*:** TEM images were acquired with a JEOL JEM2100F (JEOL Ltd.) microscope operating at 200 kV. The samples were drop-cast on 400 mesh Cu grids coated with a lacey carbon film (Ted Pella, Inc.) and dried overnight under vacuum at room temperature. The average edge lengths of the cuboidal nanoparticles were determined using ImageJ, a pixel-counting software (N = 300).

***Scanning Electron Microscopy-Energy Dispersive X-ray Spectroscopy* (*SEM-EDS*):** SEM-EDS data was obtained for elemental analysis using a JEOL JSM-7001F microscope at a working distance of 15 mm and an operating voltage of 20 kV. The samples were drop-cast on a copper substrate and dried overnight under vacuum at room temperature. For each sample, data was taken at three randomly chosen locations and averaged.

***Yield Calculation*:** The yield was calculated via thermogravimetric analysis (TGA). To determine the organic ligand content, a sample of $CsPbBr_3$ QDs synthesized in the parallel reactor after workup was heated to 500 °C under flowing nitrogen. The residual weight percent of $CsPbBr_3$ is 29%, which is then used to calculate an isolated yield of 80% based on Cs^+/Pb^{2+}.

***$CsPbBr_3$ Sizes from Photoluminescence Data*:** The resulting sizes of the pooled $CsPbBr_3$ QDs from 1, 2, 3, and 4 h were calculated using the PL emission peaks at λ_{max} = 515, 514, 513, and 513 nm, respectively.[1] From the PL data, the sizes of the QDs from 1, 2, 3, and 4 h were determined to be 11.5, 11.1, 10.8, and 10.8 nm, respectively.

A-3. Equipment and devices in the millifluidic reactor

***Flow Distribution*:** 3D-printed manifolds (inner diameter = 1.6 mm, Somos WaterShed XC 11122 photoresin) were custom-manufactured by Protolabs. Small inner diameter (ID) PEEK tubing (0.007-inch (178 μm) ID 3-inch length, and 0.005-inch (127 μm) ID 9-inch length) and the main channel PTFE tubing (1/16-inch (794 μm) ID 1-foot length) were purchased from McMaster. PEEK T-junctions with 0.020 inch (508 μm) through hole (P-712) were purchased from IDEX Health & Science. Inlet filters for the liquid streams were stainless steel mesh (# 100, 0.1-mm hole, 150- μm wires, 30% open area), and inlet filter for the gas stream was PTFE membrane filter (1.0- μm pore size, Pall Corporation). Compressed N_2 was used to apply positive pressure and displace liquid precursors, the nitrogen gas was sent into a multichannel pressure regulator (MFCS™-EZ, Fluigent), and dispensing pressures were controlled by the regulator. [**Note:** The small-bore T-junctions should be cleaned thoroughly after intense use, solid can build up after repeated use.]

***In-situ Monitoring*:** The 405 nm LED light source (M405FP1) was purchased from Thorlabs. The deuterium/halogen light source (DH-2000) and the spectrometer (FlameS) were obtained from Ocean Optics. The IR sensor (SEN-00241, 940-nm, 75-mW Emitter/Detector kit) was purchased from SparkFun. 3D-printed detection modules (RenShape SL 7820 photoresin) were custom-manufactured by Protolabs. SMA-SMA fiber patch cable (M92L01) and 1-to-4 fan-out fiber patch cable bundle (BF42HS01) were obtain from Thorlabs. The optical switch was fabricated with optical cage systems from Thorlabs, solenoids (ROB-11015, SparkFun) were integrated in the cage systems to block light from the channels that are not being read. The linear stage (MOX-06-400) was purchased from Optics Focus. Arduino boards (Uno R3, Mega 2560 R3) were purchased from SparkFun. [**Note:** When designing the optical detection modules, the optical fibers should be placed as close to the reactor channels as possible.]

A-4. Example spectra collection

The example results for parallel slugs and parallel synthesis without optimization (corresponding to Figures 2, Figure S6, Figure S7, and Table S2) were recorded with a driving pressure of 400 mbar for the Cs^+/Pb^{2+} precursor, 300 mbar for the Br^- precursor, and 400 mbar for nitrogen. Slug frequency and slug size

(ms/drop) were processed according to the voltage signals from the IR sensors installed on the 16 channels. UV-vis and PL spectra were acquired from 16 channels serially. To examine the contribution of the small diameter PEEK tubing in parallel flow, and to demonstrate that product consistency depends on well controlled driving pressures, we replaced the small diameter PEEK tubing with larger diameter (794 µm) tubing in the Br^- precursor stream. PL spectra and slug behavior were recorded under the same conditions of driving pressures.

A-5. Disturbance introduction in the reactor system

A flow disturbance was introduced into the reactor system to test the robustness of the self-optimizing algorithm. A frit filter (10 µm, A-425, IDEX Health & Science) was installed as an additional flow resistance in the Br^- precursor stream. To introduce the disturbance, manual shut-off valves (P-782, IDEX Health & Science) were used to switch the stream from bypassing the frit filter to flowing through it.

A-6. Feedback-control system

The control system was built with Python 3.6. The integrated code of this feedback-control process is on GitHub: https://github.com/LuWang04/python-mfr-feedback-control.

Table S1. Communication and control approaches for the devices used in the reactor.

Devices	Functions	Methods to achieve the functions
405 nm LED	Turn on/off	Arduino digital output
Deuterium-halogen lamp shutter	Turn on/off	Arduino digital output
Solenoids in optical switches	Turn on/off	Arduino digital output with supplementary circuit
IR sensors	Read IR receiver voltage	Arduino analogue reading with supplementary circuit
Linear stage	Transport stage to designated locations	Driven by a NEMA-23 stepper motor driver; Arduino digital signals were sent to the driver
Arduino boards	Send digital signals and read analogue signals	Communicated with a python interface pyFirmata https://pypi.org/project/pyFirmata/
Fluigent MFCS™-EZ regulator	Set and read pressures	The equipment communicates with PC through a USB cable, Python package is available in MFCS series Software Development Kit (SDK)
FlameS spectrometer	Read spectra	The equipment communicates with PC through a USB cable, Python package was obtained from https://github.com/ap--/python-seabreeze

The self-optimization procedure is illustrated in Figure S1a. The initial pressure sets were defined in the Nelder-Mead.py file. The PL and UV-vis spectra were processed in real time with Python. Emission peak wavelengths and full widths at half maximum (FWHMs) of the PL spectra were used in feedback control. The upper endpoint of 95% confidence interval (UCI) of the 16 FWHMs was minimized with the Nelder-Mead simplex method, and the optimization stopped when UCI < 35 nm. The driving pressure for either liquid precursor (P_{liq}) was ensured to be larger than 400 mbar to maintain a high throughput.

The procedure of collecting spectral information through the 16 channels is presented in Figure S1b. The slug feature data were collected from IR sensors simultaneously through multithreading. Voltages across 16 IR receivers were selected by a multiplexer in sequence and read by Arduino analogue pin. IR receivers were recorded with a time interval of 1 ms. Slug frequencies were acquired and the time lapse for each liquid slug passing the sensor was regarded as slug size in terms of time (ms/drop). IR signals were processed off-controller in real time with Python.

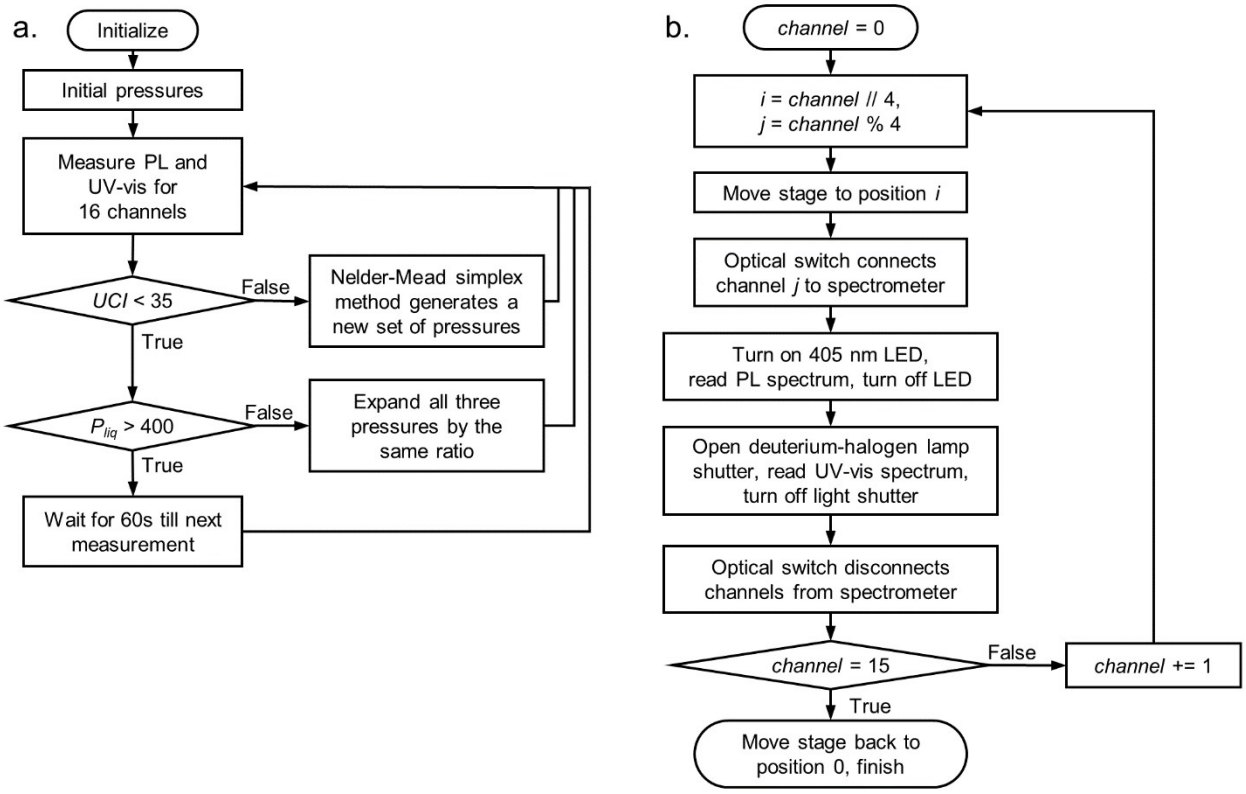

Figure S1. Flowcharts of the feedback-control process. (a) Self-optimization procedure in the parallel millifluidic reactor. UCI denotes the upper endpoint of 95% confidence interval of FWHMs in 16 channels, and P_{liq} corresponds to the driving pressure of either liquid precursor. (b) The procedure of collecting UV-vis and PL spectra through 16 channels. The spectra were read through *channel* = 0 to *channel* = 15, *i* denotes the location of the linear stage and *j* denotes the channel to be read in the 4-channel detection module.

B. Additional Supporting Figures and Tables

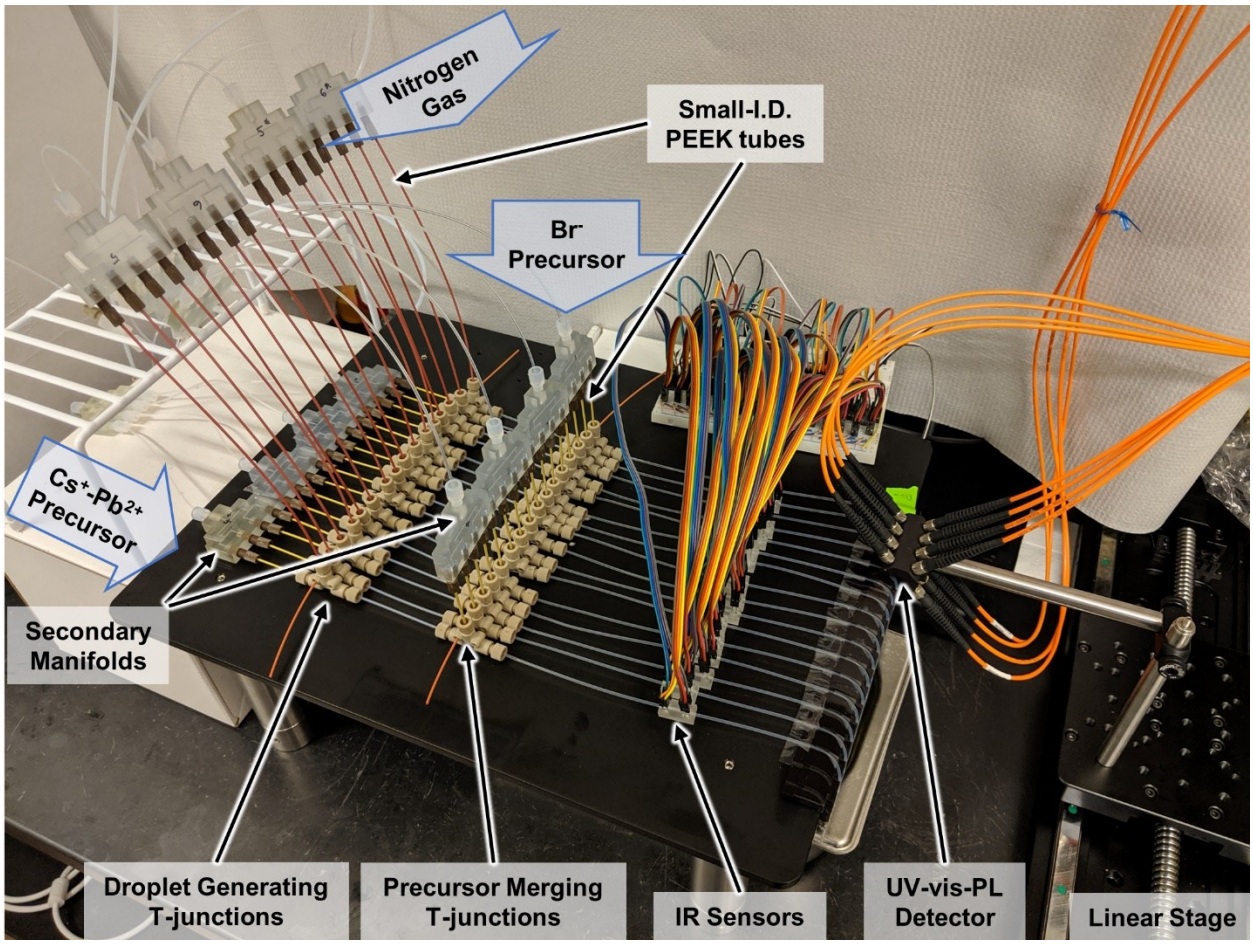

Figure S2. Photograph of the 16-channel parallel millifluidic reactor. Blue arrows indicate the flow streams.

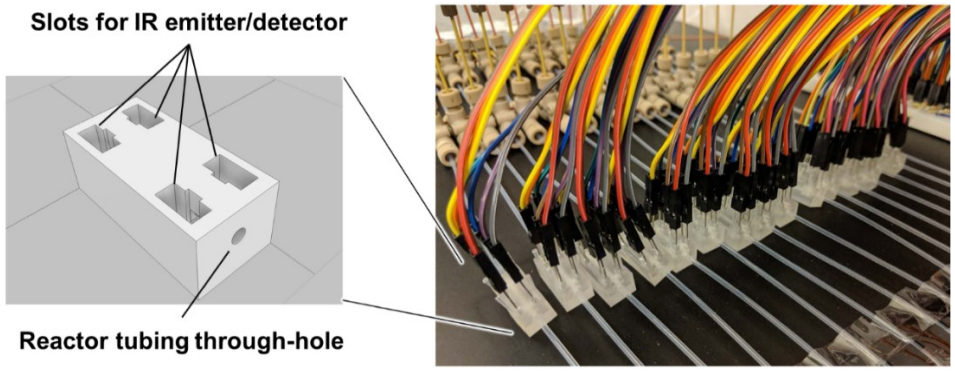

Figure S3. Diagram and photograph of the IR sensor apparatus.

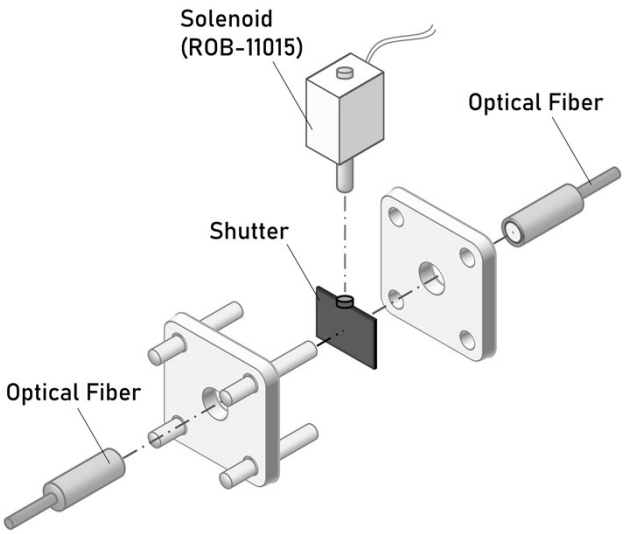

Figure S4. Exploded view of the optical switch module. Light signal from 4 channels was delivered to the spectrometer through a 1-to-4 fan-out optical fiber and light paths were switched open or closed by four of the modules. These optical switches were put inside a dark box to eliminate ambient light. When the solenoid is at rest position, the shutter covered with black masking tape isolates the light path, whereas the energized solenoid lifts the shutter to unblock the light path.

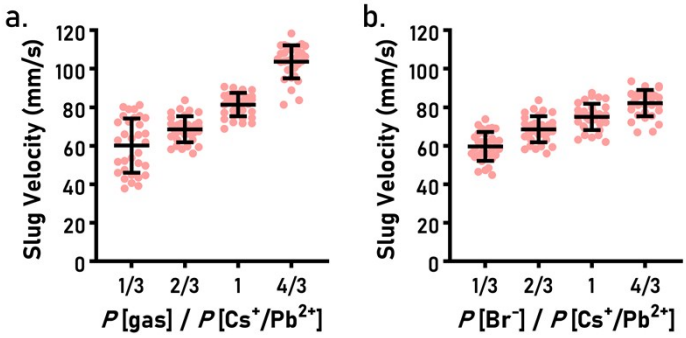

Figure S5. Slug flow rates in 16 parallel channels. The parallel slug flow was recorded by an iPhone SE in SLO-MO mode. The 240 fps videos were then processed with Fiji[2] to determine the velocity of the slugs in each channel. Slug velocities were measured with the driving pressure of Cs^+/Pb^{2+} precursor kept constant while other pressures varied. The driving pressures of Cs^+/Pb^{2+} precursor, Br^- precursor, and N_2 segmentation gas are denoted as $P[Cs^+/Pb^{2+}]$, $P[Br^-]$, and P[gas], respectively. When high and low ratios of P[gas]/ $P[Cs^+/Pb^{2+}]$ are avoided, around 8% variation can be achieved in the parallel slug velocity.

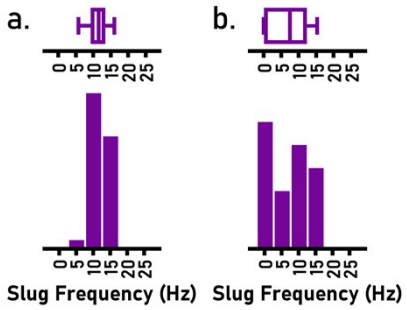

Figure S6. Box plot (top) and histogram (bottom) displaying the distribution of slug frequencies in 16 channels. (a) When small diameter (<200 µm) PEEK tubing is used to achieve parallel flow, the average slug frequency is 11 Hz and the coefficient of variance is lower than 22%. (b) When the PEEK tubing is replaced with larger diameter (794 µm) tubing, the variance of slug frequency increases to 83%.

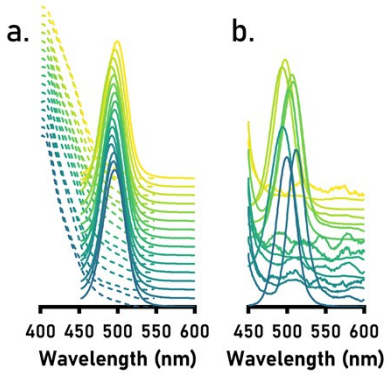

Figure S7. (a) Stacked UV-vis and PL spectra in 16 parallel channels, corresponding to the same data presented in Figure 2b. (b) When the small diameter PEEK tubing is replaced with larger diameter (794 µm) tubing, parallel flow is disrupted. Stacked PL spectra show that half of the channels do not produce PL emission, and the PL peak wavelengths in the remaining channels have a variation of 20 nm, with FWHMs variation of 10 nm.

Table S2. $CsPbBr_3$ QD synthesis was carried out in the parallel reactor (see Section A-4). Example emission peak wavelength and FWHM of the PL spectrum in each of the 16 parallel channels.

	Peak Wavelength λ_{max} (nm)	FWHM (nm)
Channel 1	496.2006	34.6923
Channel 2	494.4658	33.6668
Channel 3	495.1598	33.6624
Channel 4	491.6879	34.7460
Channel 5	492.3826	34.0423
Channel 6	493.0772	32.9896
Channel 7	492.7299	33.3433
Channel 8	495.8537	32.2618
Channel 9	496.8941	31.5599
Channel 10	496.2006	32.2618
Channel 11	494.8128	32.9726
Channel 12	494.8128	34.0117
Channel 13	491.6879	35.0912
Channel 14	494.4658	34.7147
Channel 15	496.5474	33.6450
Channel 16	499.6667	31.8798

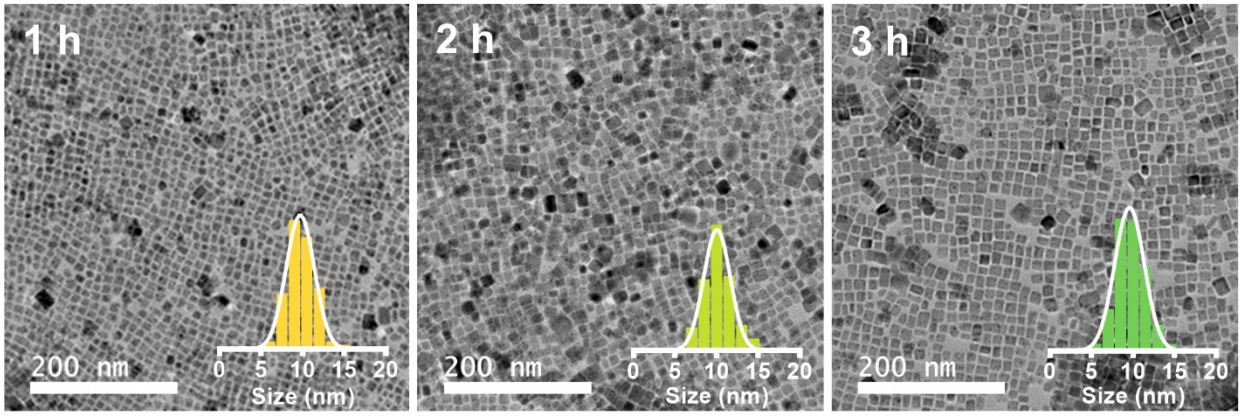

Figure S8. TEM images and inset size distributions of $CsPbBr_3$ QDs from 1, 2, and 3 h time points in the 4-h automated flow synthesis, with average sizes of 9.8 ± 1.6 nm, 10.2 ± 1.7 nm, and 9.7 ± 1.7 nm, respectively.

Table S3. Energy dispersive X-ray spectroscopic data for $CsPbBr_3$ QDs from 15 channels and pooled product from all channels after workup. The average atomic percent is presented from three distinct locations on each sample, chosen at random. Samples from 15 channels were taken, as well as a sample pooled from all 16 channels. The relative standard deviation is also presented.

Channel	Cs	Pb	Br
1	18.56	17.54	64.00
2	18.82	17.31	63.87
3	20.50	17.59	61.91
4	18.83	16.56	64.61
5	19.30	17.96	62.74
6	19.47	17.03	63.49
7	19.21	18.22	62.56
8	17.72	19.82	62.47
9	20.17	18.46	61.37
10	18.63	18.05	63.32
11	18.93	17.11	63.96
12	19.88	17.13	62.99
13	18.27	17.73	63.99
14	18.92	16.87	64.21
15	19.85	17.94	62.22
Pooled Product	19.14	16.22	63.64
Overall Average	19.18	17.60	63.27
Standard Deviation	0.72	0.85	0.99

Supporting Movie S1. A time-lapse video illustrating the trajectory of the detection module via the linear stage. The detection module is transported to 4 locations in one iteration, and at each location the detection module collects spectra from 4 channels, covering a total of 16 channels in an iteration.

Supporting Movie S2. A slow-motion video of gas/liquid slugs in the 16 parallel main channels. This video begins and ends with real-time speed, and the slow-motion portion is 4 times slower than the real speed.

C. References:

1. M. C. Brennan, J. E. Herr, T. S. Nguyen-Beck, J. Zinna, S. Draguta, S. Rouvimov, J. Parkhill and M. Kuno, *J. Am. Chem. Soc.*, 2017, **139**, 12201-12208.
2. J. Schindelin, I. Arganda-Carreras, E. Frise, V. Kaynig, M. Longair, T. Pietzsch, S. Preibisch, C. Rueden, S. Saalfeld, B. Schmid, J.-Y. Tinevez, D. J. White, V. Hartenstein, K. Eliceiri, P. Tomancak and A. Cardona, *Nature Methods*, 2012, **9**, 676-682.